Erosion Rates for Taiwan Mountain Basins: New Determinations from Suspended Sediment Records and a Stochastic Model of Their Temporal Variation

Christopher W. Fuller, Sean D. Willett, Niels Hovius,[1] *and Rudy Slingerland*[2]

Department of Earth and Space Sciences, University of Washington, Seattle, Washington 98195, U.S.A.
(*e-mail: fullercw@u.washington.edu*)

ABSTRACT

We estimate erosion rates from suspended sediment records for 11 basins in the eastern Central Range (ECR) of Taiwan using methods based on mean measured sediment discharge, a rating curve of sediment and water discharge, and a rating curve corrected for periods of limited sediment due to the lack of landslide-supplied sediment. The preferred method for any basin depends on record length and sampling frequency, with higher quality records being analyzed by the latter method. Erosion rate estimates range from 2.2 to 8.3 mm/yr for records with varying sampling frequencies and durations between 8 and 27 yr. This variation in erosion rates does not seem to reflect lithology, tectonic environment, or climate. We interpret the variation in terms of natural stochastic variation in water discharge and sediment supply. To assess the quality of the erosion rate estimates and to better understand the dependence of uncertainty on the duration and frequency of sampling, we construct a stochastic model of sediment supply and transport for the Chihpen River of the ECR. The model stochastically predicts the water discharge and sediment supply from landslides and calculates the transport of suspended sediment through application of a deterministic transport law. We determine that with a 27-yr hydrograph with 780 suspended sediment load measurements for the Chihpen River, assuming an erosion rate of 5.1 mm/yr, there is a 68.3% probability of determining an erosion rate within $\pm 2.7/4.0$ mm/yr of the actual erosion rate. We provide an estimate of the uncertainty associated with various sampling frequencies and record lengths and find that it is difficult to push uncertainties below ± 2 mm/yr.

Introduction

Suspended sediment records are commonly used as a means of estimating erosion rates in mountainous regions where the majority of eroded material is transported as suspended load. However, suspended sediment loads in mountain rivers vary dramatically with time as a result of natural variations in discharge and sediment availability. Basin-wide estimates of erosion rates are subject to large uncertainties due to this variability. Furthermore, this uncertainty is difficult to quantify since the signal variability is problematic to characterize without making measurements over a period of decades or perhaps even centuries. The quality of an erosion rate estimate is thus strongly dependent on the duration, frequency, and completeness of a sampling program (Dickinson 1981). However, it is not possible to design a sampling program or to determine its quality without understanding the causes of temporal variation in the sediment load.

The natural variation of sediment load in a river results from two sources: (1) variations in transport capacity of the river and (2) variations of sediment supply from the hillslopes to the river channel. Most sediment transport laws describe the capacity of a river to transport suspended sediment as proportional to the discharge of the river, either directly (Colby 1956) or through a velocity profile (Rijn 1984; Qiwei et al. 1989), while discharge itself is related to the rainfall within the basin and the channel network characteristics. Spatial and temporal variability of sediment supply from hillslopes to river channels is particularly pronounced in regions where the influx of sediment to rivers is in the form of discrete events such as landslides

Manuscript received September 25, 2001; accepted March 12, 2002.

[1] Department of Earth Sciences, Cambridge University, Cambridge CB2 3EQ, United Kingdom.

[2] Department of Geosciences, Pennsylvania State University, University Park, Pennsylvania 16802, U.S.A.

[The Journal of Geology, 2003, volume 111, p. 71–87] 0022-1376/2003/11101-0005$15.00

(Benda and Dunne 1997). The statistical characteristics of landslides, in particular the magnitude and frequency of their occurrence, are therefore important components of a sediment load model.

The problem of variable sediment discharge is large in regions of strong tectonic activity and high uplift rates, as this leads to accentuated relief and the predominance of deep-seated landslides as the primary mode of hillslope denudation (Anderson 1994; Schmidt and Montgomery 1995; Burbank et al. 1996; Hovius 1999). In addition, the high mountains associated with tectonic activity tend to have wet, stormy climates due to the orographic enhancement of rainfall (Barry and Chorley 1987) that leads to highly variable river discharge and an enhanced occurrence of storm-triggered landslides (Varnes 1958; Shelby 1982). Any sampling strategy that hopes to accurately estimate the erosion rate for such a region must take these supply and transport effects into consideration. For example, during any sampling period, one is likely to obtain biased rates by an oversampling or undersampling of large-scale supply and rainfall/discharge events due to the natural variation of the system.

In this article, we demonstrate the problems of sediment supply and transport and attempt to address them with respect to determining erosion rates through a statistical analysis of discharge records for a number of basins in the eastern Central Range (ECR) of Taiwan. This analysis has two parts. In the first part, we estimate erosion rates using three methods of obtaining mean sediment discharge: (1) directly from the mean of the observed sediment discharge, (2) predicting sediment discharge from water discharge using a rating curve fitted to the observed data, and (3) from a "corrected" rating curve that corrects for periods of time where the sediment load is supply limited due to the lack of landslide-supplied sediment. In the second part of this article, we construct a stochastic model of sediment supply and transport to evaluate the time variability in a sediment discharge record. Unlike some previous approaches of looking at the role of climate variability in landscape evolution (Tucker and Bras 2000), we narrow the focus by calibrating the model against hydrographic discharge data, sediment load observations, and landslide magnitude data for the Chihpen River. The model allows us to isolate the controlling factors of variable sediment supply and transport from the effects of discontinuous sampling on the uncertainty of erosion rates. In doing so, we are better able to understand the sources and magnitudes of uncertainty in the suspended sediment record.

Regional Setting

The rugged relief and high elevation of Taiwan is the result of the collision of the Luzon Volcanic Arc on the Philippine Sea Plate with the continental margin of the Eurasian Plate. Currently the plates are converging at a rate of 81.5 ± 1.3 mm/yr in a northeast direction (Yu et al. 1997). Taiwan can be divided into five regions of distinct geology and physiographic character. From west to east, these regions are (1) the Coastal Plain, (2) the Western Foothills, (3) the Hsueshan Range, (4) the Central Range, and (5) the Coastal Range. The Coastal Plain is composed of alluvial and clastic deposits shed from the uplifting Central Range. The Western Foothills are an actively deforming fold-and-thrust belt composed of Cenozoic marine and clastic shelf units (Lin 1998). The westward limit of deformation defines the boundary between the Coastal Plain and the foothills (Ho 1986). The Hsueshan Range is largely composed of the same Cenozoic marine material as the foothills, but the material has been buried and exhumed, thus exposing cleaved metasediments (Chang et al. 2000). The Central Range is divided into a western Central Range (WCR) and eastern Central Range (ECR). The WCR is a Cenozoic cover series unconformably overlying pre-Tertiary metamorphic basement that is exposed in the ECR (Lin 1998; Ho 1986). The ECR is largely composed of Mesozoic to Late Paleozoic schist and metalimestone (Ho 1986). The Coastal Range, separated from the ECR by the north-south trending Longitudinal Valley, is composed of Miocene andesitic volcanics overlain by Plio-Pleistocene flysch-type sediments and is thought to be the northern continuation of the Luzon Arc (Ho 1986; Dorsey and Lundberg 1988; Chang et al. 2000).

The rivers examined in this study are located within the ECR running transverse to the range and draining eastward to the Longitudinal Valley (fig. 1).

Hydrologic and Transport Data

Water and Sediment Discharge. The water and suspended sediment discharge records used for this study come from the Water Resources Planning Commission of Taiwan (WRPC 1972–1997). The records consist of daily water discharge measurements (m^3/s) and sporadic suspended sediment load measurements (t/d). The longest record spans 27 yr, and the highest sediment sampling frequency is 44 samples per year (table 1). No information is given

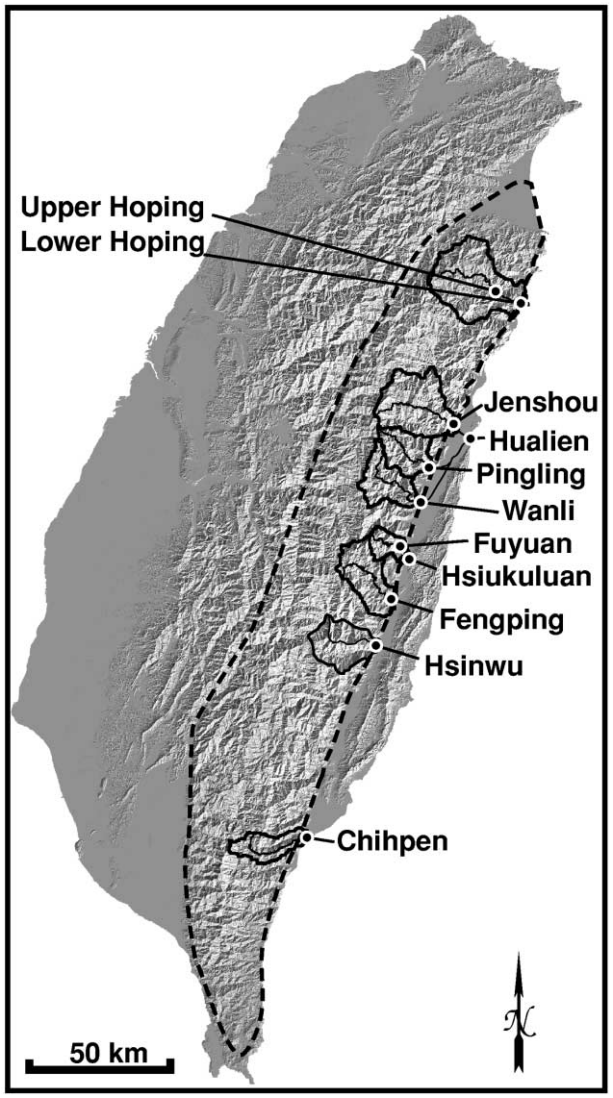

Figure 1. Topographic relief map of Taiwan showing location of rivers with basins (*solid lines*) and gauging stations (*dots*) used in this study with the outline of the Central Range (*dashed line*).

in the WRPC records with regards to the sampling methods.

A section of the time series for the Chihpen River shows two characteristics of ECR rivers as identified by Hovius et al. (2000; fig. 2). Within the time series are periods when sediment and water discharge are strongly correlated, implying a sediment surplus in the river such that the river appears to transport sediment to its capacity. In other words, during this period the sediment discharge is transport limited: the amount of sediment transported by the river is limited by the ability of the river to suspend and carry sediment. At other times, in spite of variations in water discharge, the measured suspended sediment discharge is near zero. During these periods, sediment transport is described as supply limited, since the sediment discharge, or lack thereof, appears to be limited by the availability of sediment for stream transport.

These characteristics of ECR rivers can be examined further by looking at the variation in sediment discharge as a function of water discharge (fig. 3). Two distinct fields can be distinguished in the figure. The first, characterized by finite water discharge with limited or no sediment load, represents days where the river lacked material to transport as suspended sediment (also identified as the supply-limited periods of fig. 2). The second field shows the strong correlation between water and sediment discharge identified in figure 2 as transport-limited behavior.

The dual transport-limited and supply-limited behavior of the ECR rivers can be explained in terms of sediment supply to channels in the form of landslides. Landslides produce discrete and infrequent sediment supply to a channel. Once material has been supplied to the channel, it remains available for transport until the channel has been swept clean. As the channel is being cleared, we observe a discharge record that is characterized as transport limited. Between landslides, while the channel is relatively free of suspendable material, the discharge record is characterized as supply limited. All the records for the 11 rivers in the ECR considered in this study have these characteristics.

Also evident in figure 3 is a threshold value of water discharge (~25 m^3/s) above which suspended sediment is always observed at the gauging station. This suggests that the presence of sediment, and thus landslides, is dependent on rainfall in the basin, since high rainfall produces high discharges and thus, apparently triggers landslides.

Landslide Magnitude Frequency. With the understanding that temporal variations in landslides influence the amount of sediment supplied to a river at any given time, it is important to be able to characterize the distribution of landslides within basins. Stark and Hovius (2001) demonstrated that landslide magnitudes in the ECR exhibit power-law distributions. They determined the probability density function (PDF) of 1007 landslides in the Hualien basin to have a slope of −2.112 (fig. 4). Since this distribution was determined from a single set of aerial photographs, there is no temporal constraint on the landslides, and only relative frequencies are known.

In addition to the need for temporal control to calculate mass flux from landslide frequency, it is

Table 1. Characteristics of Water and Sediment Discharge Records for Rivers Used in This Study

River	Drainage area (km^2)	Annual runoff (10^6 m^3/yr)	Length of record (days)	Days with sediment observations	Days without measurable sediment	Erosion rate from mean sediment discharge (mm/yr)	Erosion rate from rating curve (mm/yr)	Erosion rate from corrected rating curve (mm/yr)	Erosion rate from Li (1976) (mm/yr)
Chihpen	166	386.17	9862	780	364	9.5	5.2	5.1	3.7
Lower Hoping[a]	533	1138.94	5843	476	127	4.9	21.4	21.3	7.4
Pingling[a]	213	469.42	5890	513	254	3.7	26.7	26.0	5.6
Jenshou	426	815.61	9496	790	602	5.6	6.2	5.6	6.8
Hsinwu[a]	639	1472.6	3652	276	141	3.5	1.1	.9	3.8
Hsiukuluan	1539	3211	7671	613	458	7.1	8.5	8.3	3.6
Hualien	1506	2819.9	7671	616	470	10.2	2.5	2.2	4.4
Wanli[a]	242	394.15	5842	498	411	5.1	.88	.77	7.9
Fengping[a]	249	583.41	3653	304	246	5.2	2.2	1.6	…
Fuyuan[a]	56	207.61	2922	246	224	3.3	…	…	…
Upper Hoping[a]	190	399.68	5043	620	585	3.5	…	…	7.4

[a] Short records (length <6000 d and sediment observations <550 d) where the mean sediment discharge method should be used to estimate erosion rates.

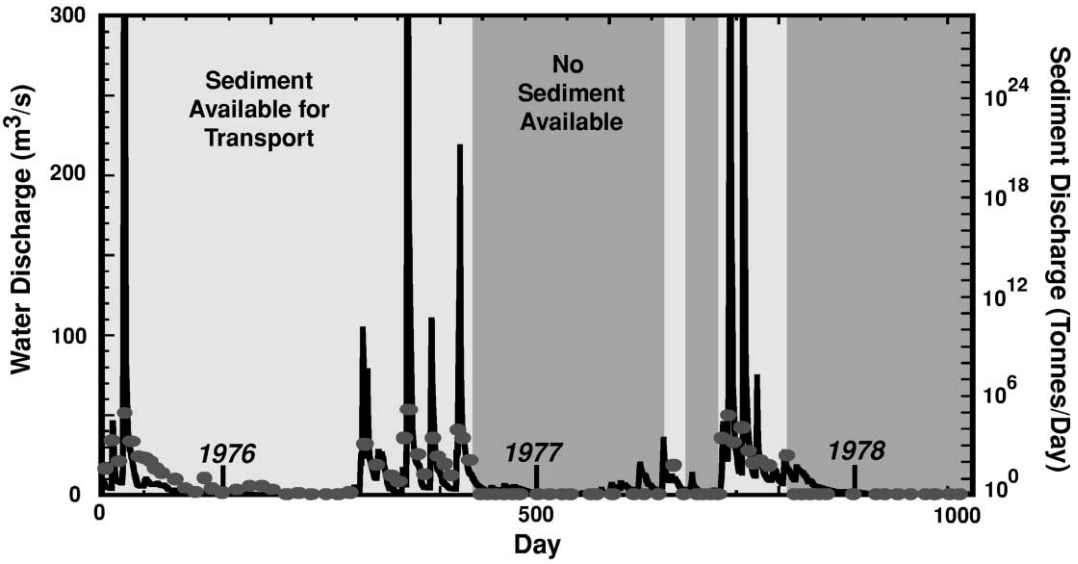

Figure 2. Representative 1000-d time series of water (*solid line*) and sediment discharge (*dots*) for the Chihpen River from July 1975 to 1978. Note periods of sediment availability, characterized by a strong correlation between water and sediment record. The hydrograph shows a strong annual periodicity due to seasonal variations in rainfall.

necessary to relate landslide area to volume. Hovius et al. (1997, 2000) use a linear square root (area)–depth relationship for landslide scars to estimate volume from the scarp area. Using this relationship, the PDF for landslide volume based on the empirical relationship for landslide area can be written as

$$P(V) = \frac{2\alpha_a A_{\min}^{\alpha_a}}{3[1 - (A_{\min}/A_{\max})^{\alpha_a}]\varepsilon^{-\alpha_a(2/3)}} V^{(-2\alpha_a/3)-1}, \quad (1)$$

where $-(\alpha_a + 1)$ is the slope of the landslide area PDF, $A_{\min}$ and $A_{\max}$ are the minimum and maximum value of landslide area described by the PDF, and ϵ is a width-depth scaling coefficient used to relate slide area to volume. Following Hovius et al. (2000), we use an ϵ value of 0.05. Equation (1) is a truncated Pareto function that we formulate to have a minimum and maximum value. Both of these values are problematic to obtain for landslide area, and their determination is described below for the Chihpen River.

Determination of Erosion Rates

Previous studies have estimated erosion rates for Taiwan from suspended sediment data. The WRPC determined an average erosion rate of 5 mm/yr for all of Taiwan (WRPC 1973). The length of the record used and the method of determination are not reported by the WRPC. Li (1976) also used data from the WRPC to determine an average erosion rate of 5.5 mm/yr from suspended sediment for the Central Range. He used a rating curve technique to approximate the relationship between sediment and water discharge and applied it to water discharge records. The quality of the record with which the rating curve parameters were determined is unknown, as is the method of determining the parameters and averaging erosion rates over the range. Li (1976) also reports erosion rates for individual basins (table 1).

With the data set provided in the more recent WRPC yearbook (WRPC 1972–1997), we have determined erosion rates for 11 rivers of the ECR by three methods: (1) using a mean sediment discharge calculated directly from sediment discharge records, (2) using a rating curve determined from the sediment discharge records applied to corresponding water discharge records, and (3) using a rating curve with sediment discharge corrected for periods of no sediment supply.

Erosion Rates from Mean Sediment Discharge. The mean sediment discharge for each river is determined by averaging the recorded sediment load values over the number of sediment observations and the time period of these observations. Depending on the river, this mean is determined from a maximum of 780 observations for the Chihpen River and a minimum of 246 observations for the Fuyuan River. The catchment-averaged erosion rate is then

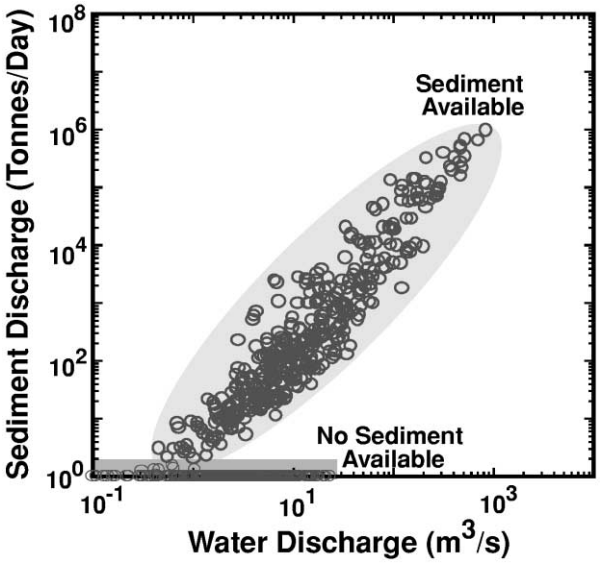

Figure 3. Water and sediment discharge for the Chihpen River. The record contains 780 measurements over 29 yr. The data on the horizontal axis represent samples, with no sediment load plotted at 1 t/d for convenience. Classifications of sediment availability corresponding to figure 2 are indicated with shading. Note the water discharge level (~25 m^3/s) above which there is always suspended sediment in the river.

determined by normalizing by the basin area upstream from the gauging station (table 1).

Erosion Rates from the Rating Curve Method. Rating curve methods use the relationship between water and sediment discharge in order to estimate sediment loads from the more complete water discharge records (Inman and Jenkins 1999). The rating curve we use here has the form

$$Q_s = aQ_w^b, \tag{2}$$

where Q_s is the sediment discharge, Q_w is the water discharge, and a and b are the rating curve parameters. These parameters are determined individually for each river from a regression of the water and sediment discharge, excluding data from days with no observed sediment discharge. Applying equation (2) to a full-length water discharge record and averaging with time and basin area gives an erosion rate (table 1). Using the rating curve method to determine an erosion rate should provide a better estimate than the mean sediment discharge method because it uses the additional information in the water discharge record. However, in doing so it assumes that the river is always transport limited as there is a unique sediment load for each value of water discharge. Since ECR rivers are not strictly transport limited (fig. 2), we expect that these erosion rates are biased toward higher values.

Erosion Rates from the Corrected Rating Curve Method. In order to correct for the transport-limited assumption of the rating curve, we also determine erosion rates using a modified or corrected rating curve. We represent the PDF of all water discharge events (fig. 5*a*) as two populations: days where there is measurable sediment load, corresponding to transport-limited days, and days where there is no measurable sediment load, corresponding to supply-limited days. These populations have PDFs $P(Q_{corrected})$ and $P(Q_{zeros})$, respectively (fig. 5*b*). A conventional rating curve, as described above, uses both of these populations to determine a mean sediment discharge. To account for the lack of sediment on days represented by the $P(Q_{zeros})$ portion of the record, we apply the rating curve only to the population of days that have measurable sediment discharge ($P[Q_{corrected}]$).

Using the general rating curve (eq. [2]) and identical parameters, we transform the $P(Q_{corrected})$ distribution of water discharge into a PDF of sediment discharge. We then calculate the expected value of this PDF. The expected value is the mean sediment discharge, assuming $P(Q_{corrected})$ describes the entire

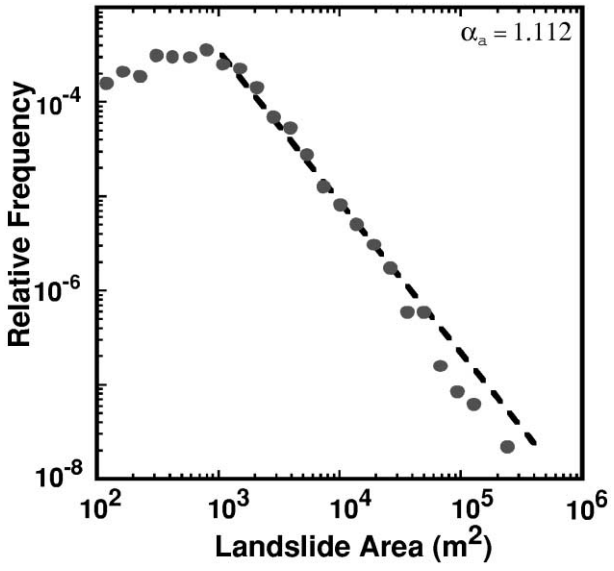

Figure 4. Relative frequency of landslides of a specific area for 1007 landslides mapped in the Hualien basin. The best-fit power law, as reported by Stark and Hovius (2000), is shown as the dashed line with a slope of $-(\alpha + 1)$, where $\alpha = 1.112$. We viewed the falloff at lower magnitudes as a sampling bias and did not attempt to model it.

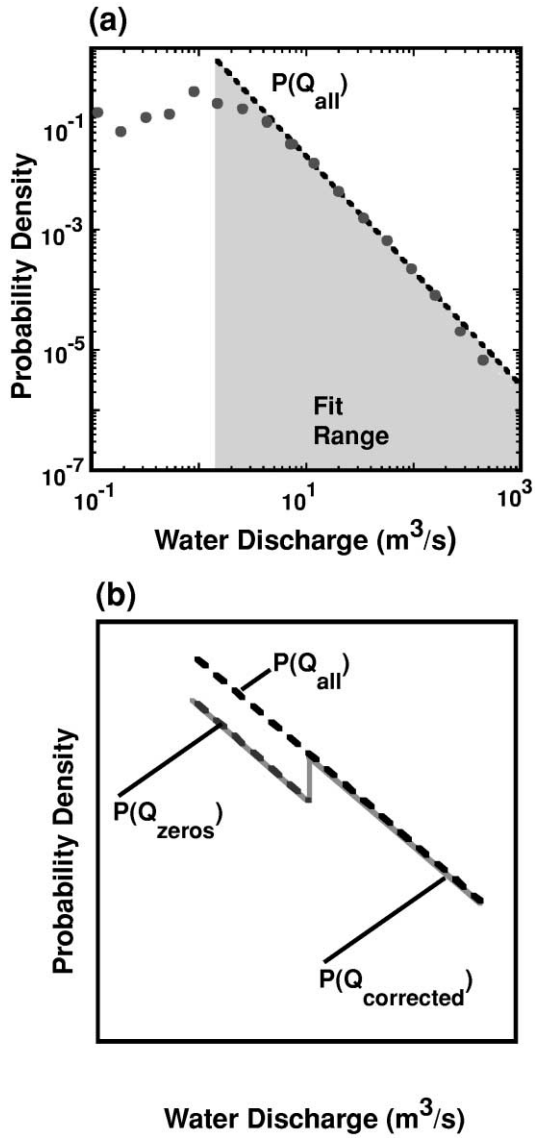

Figure 5. *a*, The water discharge record represented as a PDF ($P[Q_{all}]$) for the Chihpen River. In the figure, the PDF (*dashed line*) is above the binned events (*dots*), suggesting a misfit to the data. This apparent misfit is due to the PDF having been fit only to the renormalized discharge events within the fit range. *b*, $P(Q_{all})$ from *a* decomposed into days with no corresponding sediment load, $P(Q_{zeros})$, and days with sediment present, $P(Q_{corrected})$. The corrected rating curve method of determining erosion rates relies on determining a mean sediment discharge by transforming $P(Q_{corrected})$ to a PDF of sediment discharge using equation (2). See text for details.

record. To account for the days without sediment discharge, we scale the expected value by the fraction of days where measurable sediment has been recorded over the total number of days with sediment observations. Dividing by the basin area yields the erosion rate (table 1). Although this method takes into account the probability of the river being transport limited, it is problematic in application because it requires sufficient data to accurately estimate the PDF for supply-limited days, $P(Q_{zeros})$, and the PDF for transport-limited days ($P[Q_{corrected}]$).

Results

The erosion rates determined from the three methods above are presented in table 1. Due to the small number of days with sediment discharge, the rating curve and corrected rating curve methods were not used on the Fuyuan or Upper Hoping records. Erosion rates from the mean sediment discharge method are fairly consistent throughout the basins, with the majority of the rates around 3–5 mm/yr. The Hualien and Chihpen Rivers are exceptions with inferred erosion rates of 10.2 and 9.5 mm/yr, respectively. Erosion rates from the rating curve method are generally lower, but there are some outliers: the Lower Hoping and Pingling Rivers have an erosion rate almost an order of magnitude greater. As expected, the corrected rating curve rates closely mirror the rating curve rates with slightly lower values due to the correction for periods without any sediment discharge.

With the corrected rating curve method, the Lower Hoping and Pingling Rivers yield estimates greater than 20 mm/yr, more than three times higher than neighboring basins. While these values could reflect differences in basin characteristics, we believe it is more likely that the relatively high estimates are a consequence of the inability to effectively determine a rating curve with short, incomplete data sets. The exact criterion that determines when rating curves are effective is not investigated here, but we believe that the rating curves used here are accurate enough to produce meaningful results when the record length is greater than 6000 observations and the number of sediment observations is greater than 550. Rivers that do not meet these criteria (footnoted in table 1) should be evaluated using the mean sediment discharge method.

Stochastic Model of Sediment Supply and Transport

Many authors have addressed the uncertainties in determining erosion rates from suspended sediment records (Branski 1981; Dickinson 1981; Walling and Webb 1981). Analyses like these are essen-

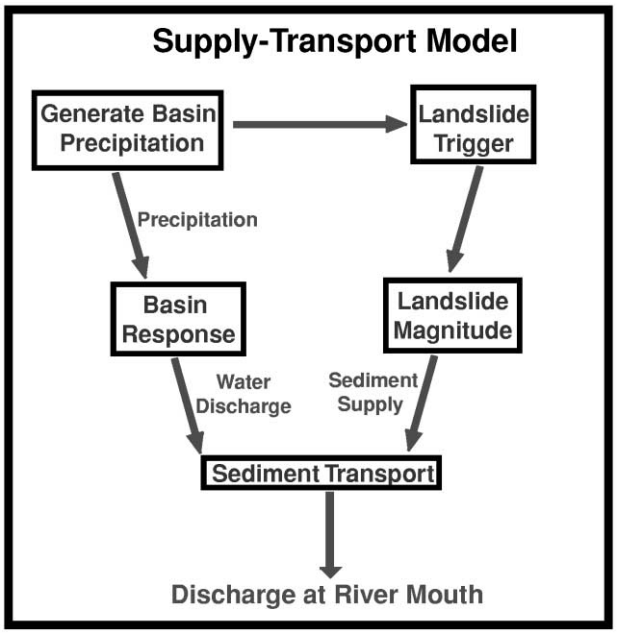

Figure 6. Major components of the sediment supply and transport model. See text for details.

tial to understanding the accuracy and precision of the estimated erosion rates, given the absence of continuous sediment discharge records and because of the difficulties associated with highly variable sediment discharge. We take this type of analysis one step farther and investigate how the causes of the variability in sediment records affect the uncertainties in erosion rates. In this section, we develop a model of sediment supply and transport that includes the two main physical sources of sediment variability: (1) temporal variations in the rainfall and thus variations in water discharge and sediment carrying capacity and (2) variations in sediment supply, which is assumed to be landslides. We incorporate two stochastic components into our model, one for rainfall and one for landsliding, and couple them to a deterministic model for sediment transport to test how these factors influence the observed variability in sediment discharge and thus estimated erosion rates. A basic outline for the model is shown in figure 6. Synthetic rainfall for the basin is generated from a power law PDF describing the daily frequency of rainfall for a given magnitude. We use the rainfall to determine the water discharge, suspended sediment transport capacity for the river and as a triggering mechanism for landslides. The magnitude of landslides is determined from a PDF describing the magnitude-frequency relationship of landslide volume. Slide material is deposited in the stream channel and is transported out of the basin according to the capacity determined from the water discharge. We calibrate and apply this model to the Chihpen River of the ECR. The Chihpen was selected due to the quality and duration of the water and sediment discharge record.

Water Discharge. We do not have rainfall data for the Chihpen basin, so we must infer the amount of rainfall from the hydrograph. We treat the hydrograph for the Chihpen River as a sequence of rainfall impulses to the basin convolved with a basin response to rainfall events. The basin response function is used to deconvolve the hydrograph generating a time series of "rainfall events," which we use to determine the PDF of rainfall. We do not expect the deconvolved hydrograph to equate to rainfall records. It is only a proxy for rainfall within the basin that allows us to generate random, yet realistic hydrographs. For this reason, the rainfall events have the same unit as the hydrograph: m^3/s. Given this PDF, the stochastic component of our model produces a synthetic record of rainfall events that are convolved with the basin response to determine a synthetic discharge record.

The water discharge record is observed to have three distinct time scales of discharge in response to a rainfall impulse (Pearce and McKerchar 1979), and these comprise the basin response function. We determine a three-part exponential to this impulse response for the Chihpen River (fig. 7) that takes the following form:

$$Q(t) = Q^* \exp(-\mu_i t), \tag{3}$$

where Q is the water discharge, Q^* is the impulse, t is the time in days since the impulse, and μ_i is the scaling constant. The scaling constant is .85 for the first 2 d, .35 for the following 6 d, and .05 for the next 200 d. The standard deviation of the misfit between the original hydrograph and the reconvolved hydrograph is 2.6 m^3/s.

There are two discernible seasons of water discharge for rivers in the ECR (fig. 2). These seasons are related to the annual shift from a northeasterly monsoon in the winter to a wetter southwesterly monsoon in the summer months marked by the beginning of the Mei-Yu in mid-May (Ramage 1971; Tao and Chen 1987; Chen et al. 1999). To account for this annual variation, we group the deconvolved hydrograph into two populations referred to as the dry and wet seasons. The rainfall events are binned

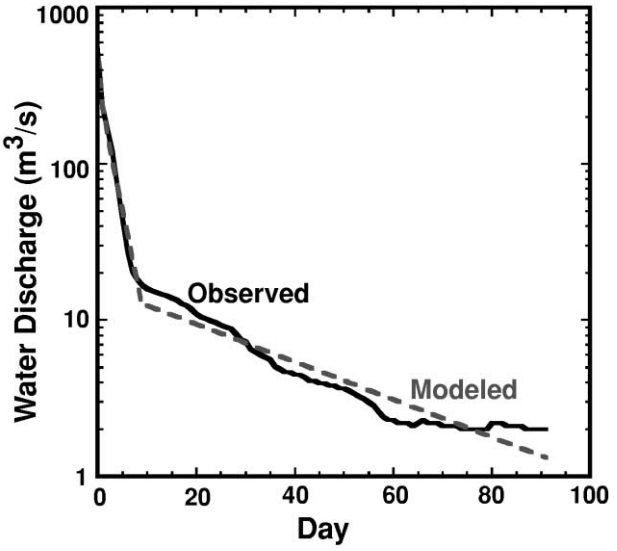

Figure 7. Typical basin runoff response for the Chihpen River, beginning August 15, 1982, and the basin response used in the model. The response model is a three-part exponential described by equation (3); duration is 208 d.

in their respective groups, and to this distribution we fit a truncated Pareto function of the form

$$P(Q^*) = \frac{2\alpha_p R_{\min}^{\alpha_p}}{1 - (R_{\min}/R_{\max})} Q^{*-\alpha_p-1}. \quad (4)$$

We chose a truncated Pareto because it allows us to specify maximum and minimum bounds for the distribution. For each PDF (eq. [4]), we found Pareto parameters of $\alpha_{pw} = 0.6$, $R_{min,w} = 0.805$, and $R_{max,w} = 563.0$ (wet season), and $\alpha_{pd} = 1.05$, $R_{min,d} = 0.805$, and $R_{max,d} = 1000.0$ (dry season). The slopes of the distributions $(1 - \alpha_p)$ are determined from a least-squares fit to the deconvolved hydrograph for each season. The maximum value (R_{max}) is set to the size of the maximum observed rainfall event for the basin during the respective season, and the minimum value (R_{min}) is chosen so that the expected value of the PDF is equal to the mean rainfall event. The high dry season maximum relative to the wet season might be accounted for by the passing of a late fall typhoon (Nuttonson 1963).

To generate a synthetic discharge record, we first generate a synthetic distribution of rainfall through random sampling of the PDF combined with the probability of rainfall occurring on any given day. The probability of rainfall for any day is determined for each season as the fraction of days where the deconvolved hydrograph is above the minimum value reported above. Random sampling of any PDF is described by

$$E = P^{-1}(x), \quad (5)$$

where E is the generated event, P is the equivalent cumulative distribution function (CDF), and x is a uniform deviate between 0 and 1 (Press et al. 1988). By repeatedly evaluating the inverse of the CDF at uniformly random values between 0 and 1, we generate a sequence of rainfall events, E, that matches the original PDF. The synthetic rainfall events generated individually for each population are combined and convolved with the basin response to calculate the water discharge at the gauging station. Water discharge upstream from the station is linearly scaled with contributing basin area accounting for all tributaries.

Sediment Supply. In the ECR, landslides exhibit a magnitude-frequency relationship that can be represented with a truncated Pareto PDF (eq. [1]; fig. 4). We use this PDF to generate synthetic landslides in the same manner as the rainfall. However, the PDF only describes relative frequencies between landslide magnitudes. In order to obtain the absolute frequencies for landslide magnitudes we define a basin-wide erosion rate as

$$\dot{e} = \frac{NE\{V\}}{A\Delta t}, \quad (6)$$

where N is the number of landslides occurring in the basin over a time period Δt, $E\{V\}$ is the expected volume of these slides from the PDF for landslide volume and A is the basin area. For this study we use an erosion rate of 5.1 mm/yr as determined from the corrected rating curve method described above for the Chihpen River. Solving this equation for N gives the number of landslides occurring in an area A over the time interval Δt. Based on the correlation between high discharge and sediment supply (fig. 3), we assume that landslides in the basin are triggered by rainfall. We introduce the influence of rainfall by scaling the expected number of slides by the ratio of the actual rainfall to the expected value of the rainfall each raised to the power β so that days with water discharge that is higher than the expected value will have more landslides:

$$N = \left[\frac{\dot{e}A\Delta t}{E\{V\}}\right] \frac{(Q^*)^\beta}{E\{(Q^*)^\beta\}}. \quad (7)$$

If, for the sake of simplicity, we treat landsliding

as a Poissonian process, the probability of n slides occurring on a given day is

$$P(n) = \frac{N^n \exp(-N)}{n!}, \quad (8)$$

where N is the expected number of landslides as defined above. We use the Poissonian probability of landsliding to determine if and how many landslides will occur and to determine the volume of those landslides from the landslide volume PDF using the same sampling method described above for rainfall.

Sediment Transport. For simplicity, we assume that all landslide material is deposited directly in the river channel and is transported as suspended sediment. We do not address material that is transported as bedload and landslide debris that is stored on riverbanks. The impact of these assumptions is lessened with the understanding that the landslide volumes we model are only those portions of the slides that are transported as suspended sediment. Therefore, the only material that is not accounted for between our model and the observed data is the bedload that is broken down to suspended sediment during transport. Landslide material is entrained up to the capacity of the river at any point. Lacking detailed hydraulic data and observations of the bed profile, we avoid using more complex methods of modeling suspended sediment transport (Rijn 1984; Qiwei et al. 1989) and revert instead to the simple representation of transport capacity as

$$K = kQ_w^b, \quad (9)$$

where k is a transport coefficient for the river and Q_w is the water discharge at the point of interest. We use a value of $b = 2.0$ that is consistent with the sediment load data from the Chihpen River (fig. 3).

Coupled Model. The fully coupled model of sediment supply and transport (fig. 6) is used in conjunction with an upstream distance, contributing area profile for the Chihpen River generated from a 40-m DEM (digital elevation model) of Taiwan. We use the DEM spacing of 40 m to define our calculation points, or nodes, for the model. Our time step for the model is 1 d, so as to match the observed sediment discharge data reported in tonnes/day.

The model calculates the water discharge in the form of rainfall events for each day. Each rainfall event is convolved with the basin response to determine the water discharge at the gauging station. Beginning at the headwaters and working downstream, the sediment input to a node is determined from the volume of material deposited from landslides directly at the node and from the transport of sediment from upstream nodes.

Sediment supply at any given node is calculated using the rainfall in conjunction with equations (7) and (8). In equation (8), we determine the probability of n landslides at the node where n varies between zero and some arbitrarily large number, usually set to 100. We then use the Poissonian probabilities to determine how many slides occur. If any slides do occur, the volume of the slides is determined from a random sampling of the landslide volume PDF (eq. [1]) for each slide. The volume of the landslide is then stored as available sediment at the node. The scaling of the expected number of landslides, N, with the contributing area (eq. [7]) allows us to take into account sediment input from tributaries.

Discharge at the node is calculated by linearly scaling the discharge at the gauging station upstream with contributing area. The sediment transport to the adjacent downstream node is equal to the capacity of the current node (eq. [9]) if the sediment at the node from previous time steps and the input of sediment from landslides and upstream transport is greater than the capacity. All material above capacity is stored in the current node for the next time step. If the sum of stored sediment and incoming sediment is less than the capacity, all of the sediment is transported to the downstream node and nothing is stored. At the end of each time step, the model suspended sediment transported past the gauging station is recorded as the sediment discharge for the day.

The model is designed to run Monte Carlo simulations. For each simulation, we vary the random number generator seed used to determine the magnitude of rainfall (eqq. [4], [5]), the number of landslides at each node (eqq. [7], [8]), and landslide magnitude (eqq. [1], [5]). Using the stochastic model, we can also produce records of any length, thus permitting investigation into the uncertainties introduced by use of shorter records. Formulating the model in such a manner allows us to investigate trends in characteristic parameters.

Model Results

The primary output from the coupled model is the water and sediment discharge at the gauging station (fig. 8). We use this information and its derivatives to calibrate the model to the Chihpen River. After calibration, we run Monte Carlo simulations for optimal parameter sets to investigate the effects of

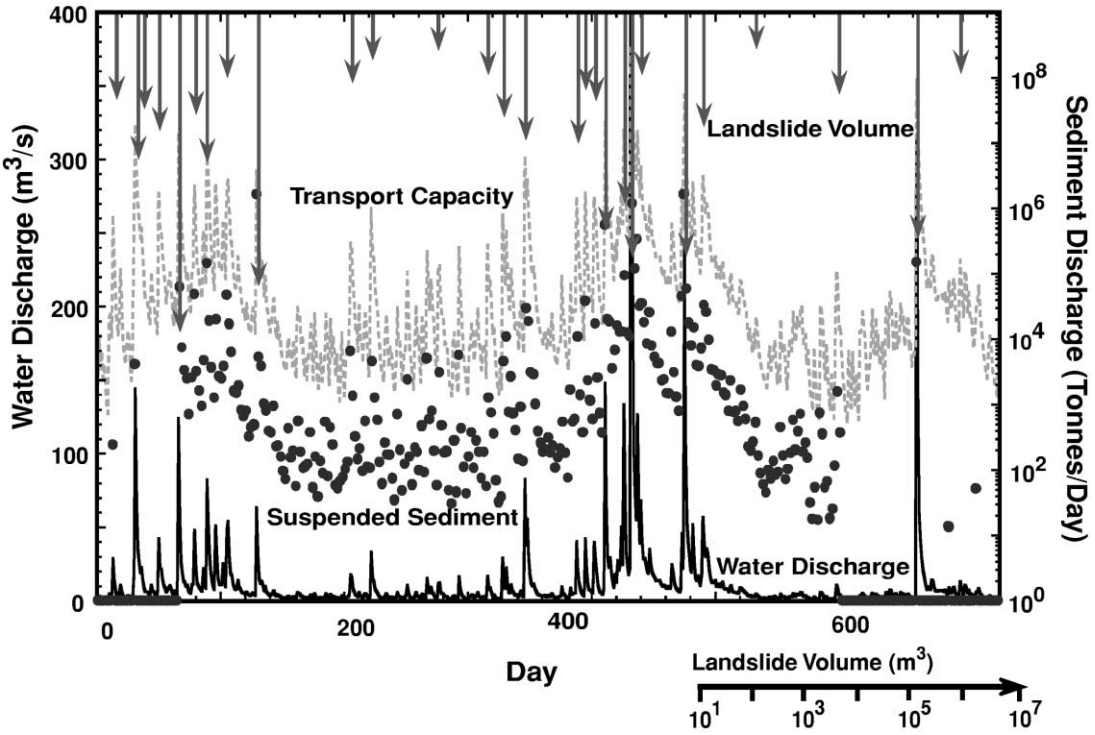

Figure 8. Typical model output contains synthetic water and sediment discharge (*solid line* and *circles*, respectively), transport capacity at the gauging station (*dashed line*), and landslide volumes (*arrows*) for the basin. For this simulation, $\beta = 2.0$, $A_{min} = 20$, and $k = 378$.

varying sediment supply and transport on the uncertainty in erosion rates determined from suspended sediment records.

The model also predicts the capacity of the river at the gauging station and the total volume of landslides for each day. The effect of representing the water discharge with two individual PDFs is apparent in the reproduced seasonal periodicity of water discharge. Also, the scaling of landslide probability with rainfall (eq. [7]) is apparent from the correlation between landslide occurrence and high discharge events. The dual transport-limited and supply-limited nature of the rivers is also apparent. As explained below, the presence of this characteristic depends on specific parameters. In particular, it depends on the balance between the river's ability to transport material out of the basin, which is controlled in turn by the transport coefficient, k, and the frequency and the amount of landslide material, which depends on the minimum landslide area, A_{min}.

Of the model parameters (table 2), only the minimum landslide area, A_{min}, the transport coefficient, k, and the landslide scaling exponent, β, are not independently constrained. We constrain the maximum rainfall, R_{max}, by fixing it to the maximum of the deconvolved hydrograph. With this fixed and the distribution slope known, we pick a minimum rainfall, R_{min}, so that the expected value of the rainfall PDF matches the mean observed water discharge.

We estimate the maximum landslide area, A_{max}, using the maximum basin relief, which does not exceed 1 km in the Chihpen basin. With this value, and assuming an elliptical landslide form (Hovius et al. 1997, 2000), we determine a maximum area of 400,000 m^2 or a volume of 1.27×10^7 m^3. We are unable to constrain the minimum landslide area, A_{min}, from field observations since we only know the relative frequency of the landslide PDF.

Since we do not have any data to constrain k, A_{min}, or β, we use Monte Carlo simulations to generate suites of models and compare observed characteristics of the record to those of the model. Each simulation in a set is run for 27 yr, the length of the observed record, with constant parameter values throughout the set. The characteristic value of interest is recorded for each simulation, and the mean and standard deviation of the value are calculated. The number of simulations in each set var-

Table 2. Model Parameters

Variable	Description
α_a	Slope of landslide area magnitude-frequency distribution
A_{min}	Minimum cutoff of landslide area magnitude-frequency distribution (m^2)
A_{max}	Maximum cutoff of landslide area magnitude-frequency distribution (m^2)
$\alpha_{pw, pd}$	Slope of rainfall event magnitude-frequency distribution for wet and dry seasons
$R_{min, w, d}$	Minimum cutoff of precipitation event magnitude-frequency distribution for wet and dry seasons (m^3/s)
$R_{max, w, d}$	Maximum cutoff of precipitation event magnitude-frequency distribution for wet and dry seasons (m^3/s)
ϵ	Width-depth scaling coefficient for landslides
$\dot{e}$	Defined erosion rate for basin (mm/yr)
μ_j	Scaling coefficients for basin response function
k	Transport coefficient for suspended sediment [ts/(m^3d)]
β	Landslide scaling exponent

ies with the parameter being investigated. Typical sets have 200–1000 simulations.

Calibration. Unknown model parameters consist of k, A_{min}, and β. The fraction of days with sediment observations that have no measurable sediment, F_z, is a useful parameterization for the frequency with which a river has measurable sediment load. We use Monte Carlo simulations with varying k and A_{min} to examine how these parameters affect the predicted F_z and to determine an appropriate combination of k and A_{min}. In order to constrain β, we quantify the effects of varying β on the triggering of landslides.

Figure 9 shows the effect of varying k and A_{min} on F_z. The figure shows the mean F_z with ± 1 standard deviation, determined from sets of 500 simulations for $\beta = 2$ and 250 simulations for $\beta = 1$. The observed F_z for the Chihpen River is also indicated. The trends can be explained in the following way. A higher k implies faster sediment removal, thereby leading to a higher fraction of days without sediment load, F_z. Increasing A_{min} in the model increases the expected value of landslide area, and thus, fewer landslides are required to match the defined erosion rate. In general, larger landslides imply less frequent sediment inputs and therefore a higher F_z. However, with very large landslides, sediment can take several years to be removed, producing a lower F_z.

As defined in equation (7), β affects the expected number of landslides for a given rainfall magnitude.

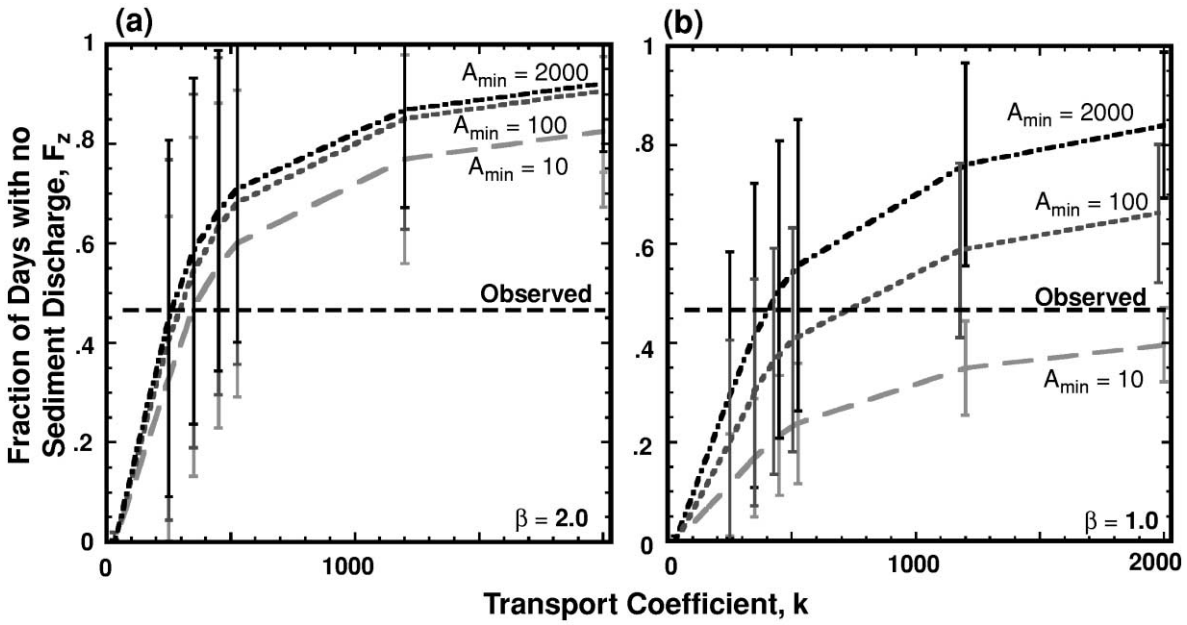

Figure 9. Variation in the fraction of days with no sediment discharge, F_z, as a function of minimum landslide area, A_{min}; transport coefficient, k; and scaling exponent, β. Error bars show the $\pm 1 - \sigma$ variation from the mean F_z determined from 500 realizations for $\beta = 2.0$ (*a*) and 250 realizations for $\beta = 1.0$ (*b*).

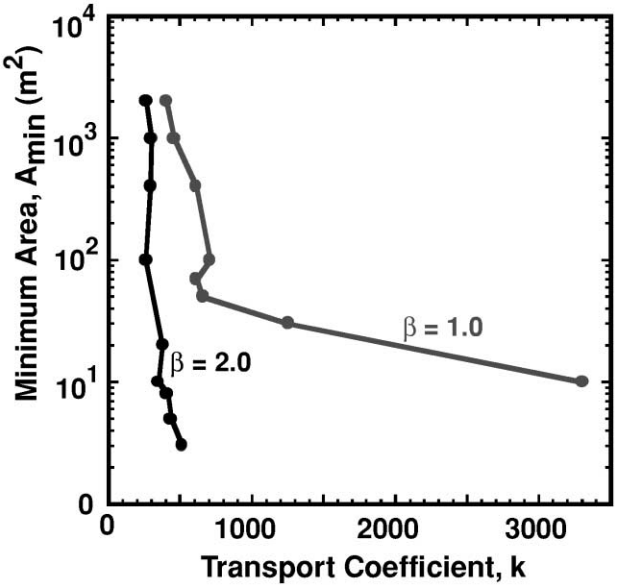

Figure 10. Acceptable sets of parameters determined from figure 9. Acceptable values are defined as the sets of β, A_{min}, and k, whose mean fraction of days with no sediment discharge, F_z, matches the observed F_z.

A high β value results in a higher number of landslides on days with high rainfall and thus discharge and transport capacity. As shown in figure 9, by lowering β from 2.0 to 1.0, higher transport coefficients are needed to match the observed F_z for a given A_{min}.

Given the results shown in figure 9, we pick two suites of k and A_{min} values, corresponding to β values of 2 and 1, respectively. The pairs are defined to be acceptable if the mean F_z of the Monte Carlo simulations equals the observed F_z (fig. 10). From the acceptable sets of values, we choose an optimum pair by assuming that the minimum possible values of both k and A_{min} are the most physically reasonable. Use of the minimum value of A_{min} is justified by the observation that landslides occur at very small scales, and we would like to simulate the small but frequent contribution of sediment from these slides. We prefer the use of a small value of k based on the observation that the water and sediment discharge data for the Chihpen River lie on a rating curve with a minimum transport coefficient of 30 $(t \times s)/(m^3 \times d)$ (fig. 11). We expect the actual transport coefficient for the river to lie somewhere above this because the river will not transport its full capacity at the river mouth unless there is a landslide directly above the gauging station (fig. 8). Therefore, we argue for a k greater than but as close to 30 as possible. Using the above reasoning leads us to chose $\beta = 2.0$, $A_{min} = 10$, and $k = 346$ as our optimal parameter set (fig. 11).

Discussion

With the calibrated model of sediment supply and transport for the Chihpen River, we are able to look at how discontinuous sampling and variations in sediment discharge affect uncertainties in erosion rates. Figure 12 summarizes the results of the Monte Carlo simulations. Figure 12*a* shows the variation in the mean erosion rate for increasing sampling frequencies. Each error bar denotes the 68.3% probability of occurrence about the mean from a set of 10,000 simulations, each having a 27-yr duration. This range is equivalent to the mean $\pm 1 - \sigma$ variation often reported for normal distributions, but in this case the distribution of erosion rates is closely approximated by a lognormal distribution resulting in an asymmetric uncertainty (Limpert et al. 2001). Note that the observed erosion rate, from the corrected rating curve, is 5.1 mm/yr. As this is prescribed in the sediment supply

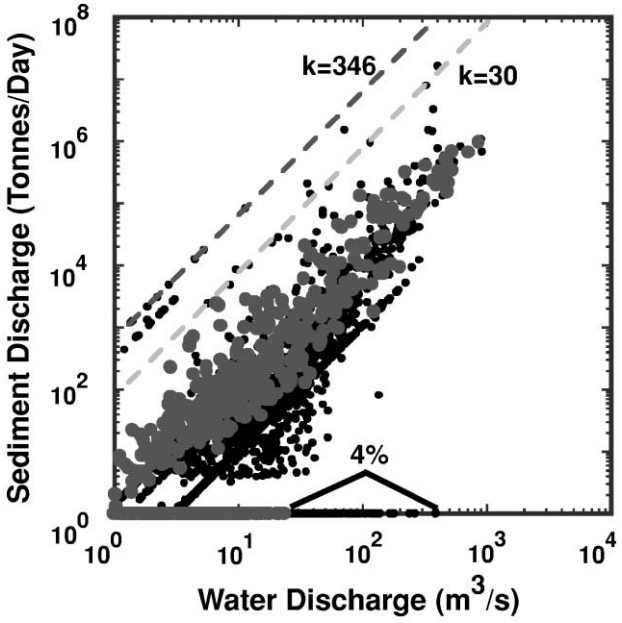

Figure 11. Predicted water and sediment discharge for a 27-yr simulation (*small dots*) overlaid with the observed record (*large dots*). The transport coefficient used in the model, $k = 346$, and the minimum transport coefficient, $k = 30$, needed to describe the observed data are shown as calculated from equation (2). The observed maximum water discharge above which there is always sediment in transport is surpassed by 4% of the model days, as indicated.

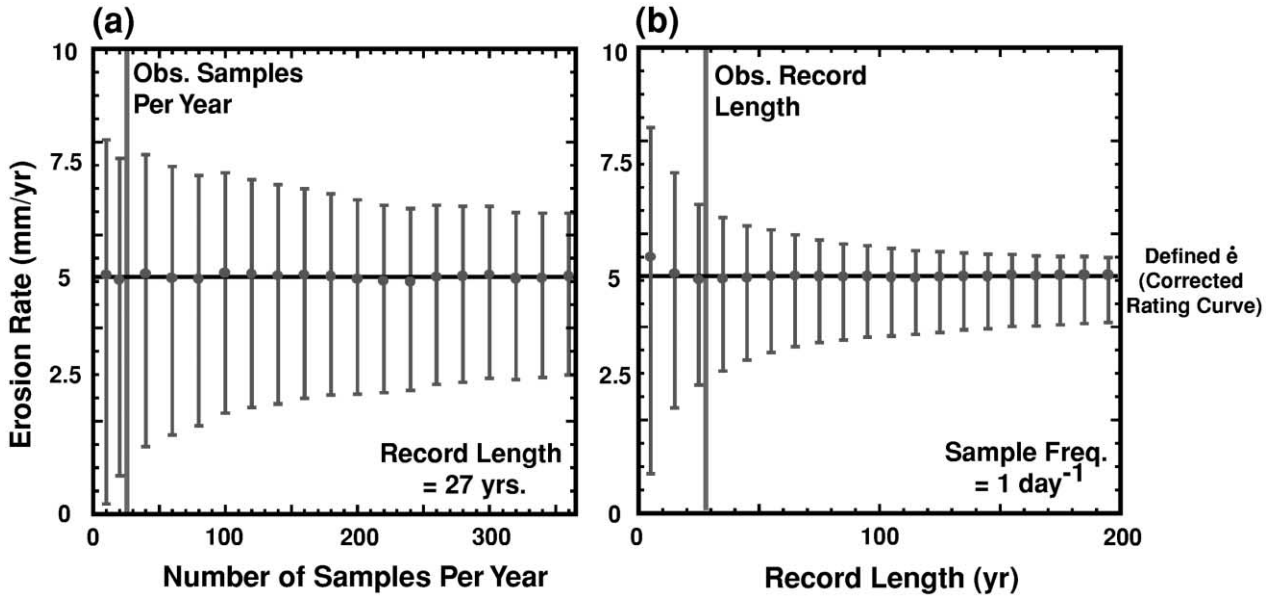

Figure 12. *a*, Mean erosion rates determined from the mean sediment discharge of 10,000 27-yr model simulations for the Chihpen River, with the 68.3% probability of occurrence interval showing a decrease in uncertainties with an increase in sampling frequency. The confidence interval of the observed sampling frequency of 29 samples/yr is ±2.7/4.0 mm/yr. The asymmetric distribution of uncertainties is due to the lognormal characteristics of the erosion rate distributions. *b*, Mean erosion rates as a function of record length determined as in *a*, but from 1000 simulations. Simulations consist of records with a sampling frequency of 1/d. With a 100-yr record and 1/d sampling frequency, the variation would be ±.6/1 mm/yr. In *a* and *b*, the solid black line indicates the erosion rate of 5.1 mm/yr used in the model.

component of the model, it is not surprising that the model reproduces this value. More interesting is the decrease in the variation about this mean as the sampling frequency increases (fig. 12*a*). As the sampling frequency approaches 1/d, the variation stabilizes to approximately ±1.4/2.0 mm/yr. This value represents the variation from discrete sediment supply and varying transport capacities for the river. The actual record of the Chihpen has a sampling frequency of 29 d/yr, so we expect the 68.3% probability range at that frequency to be ±2.7/4.0 mm/yr with contributions to the variation from both the sampling frequency and the inherent random nature of the supply and transport system.

A similar relationship is derived in figure 12*b* for the effect of record length on variance in the sediment discharge and estimated erosion rate. The sampling frequency in this set of 1000 simulations is set to 365 d/yr.

Figure 12 is useful in evaluating the accuracy of erosion rates determined from suspended sediment in tectonically active regions where sediment supply is dominated by landslides and accurately described by the above model. Assuming the Chihpen River has an actual erosion rate of 5.1 mm/yr, if we continuously sampled the suspended sediment for 100 yr, we would have 68.3% confidence that we were within ±0.6/1 mm/yr of the actual erosion rate. While this seems like reasonable accuracy in estimating an erosion rate, it is rare to have continuous records for any duration, and record lengths longer than a few decades are uncommon. Confidence levels for more realistic scenarios can be derived from figure 12.

Of interest to this study is the significance of these findings as applied to the erosion rates reported above for other rivers in the ECR of Taiwan. However, without completing the full simulation process for all of the rivers, it is difficult to estimate the uncertainty in erosion rate. The above work shows that the uncertainty depends on both observational factors, the length of the record, and the sampling frequency, as well as natural factors, the sediment supply, and rainfall characteristics. We can qualitatively extrapolate the uncertainty for the Chihpen River to other ECR rivers by looking at the difference in these factors between rivers. A river with a fairly constant sediment supply, perhaps accounted for by hillslope diffusion or contin-

uous mobilization of sediment in an alluvial channel, would have minor variations compared to a river dominated by discrete supply processes like landslides. Furthermore, among basins dominated by landslides, we would expect to see different magnitudes of variation from slight changes in the landslide distributions. With a steeper landslide area–magnitude distribution, $\alpha > 1.112$, we would see a decrease in the uncertainty since there would be fewer large landslides skewing the sediment discharge. While our initial work suggests that other basins in the ECR have similar landslide distributions, this effect should be considered when looking at other regions. Also, a smaller range in the rainfall distribution, that is, closer minimum and maximum values in the rainfall PDF, would decrease the variance in the transport capacity, thereby resulting in less variation in sediment discharge at the mouth of the river and in erosion rates. We have not investigated the potential differences in rainfall distributions between catchments, but due to the similar climate throughout the ECR, we do not expect much variation. From the above reasoning on sediment supply and rainfall characteristics combined with the fact that the Chihpen River has the longest record and one of the highest sampling frequencies of ECR rivers, we believe that the uncertainty for the other rivers will be similar or greater than that of the Chihpen River.

Using ±2.7/4.0 mm/yr as the minimum confidence interval shows that all of the ECR rivers' erosion rates, determined here using the mean sediment discharge method, are equivalent within the 68.3% confidence interval. The other methods of determining erosion rates yield consistent erosion estimates with the exception of the Lower Hoping and Pingling Rivers. There are three possible explanations for these higher rates: (1) they are real, (2) the records for these rivers oversample large sediment discharge events, and (3) with the shorter records and possibly higher erosion rates, the confidence interval for these erosion rates is much larger than for the Chihpen, making the difference in rates insignificant. In some instances, there is a large difference in the erosion rates determined from the mean sediment discharge and those from the rating curve and corrected rating curve. However, when considered with respect to the confidence interval, this difference is insignificant. Keeping in mind the magnitude of expected errors in estimating erosion rates from suspended sediment, we see that the erosion rates determined here are also consistent with the work of Li (1976).

It is important to recognize that the erosion rates determined here do not take into account material transported as bedload. Studies of sediment transport in other regions vary widely in their estimations of the fraction of total sediment transport from bedload, anywhere from 10% to 50% of the total load (Nanson 1974; Williams and Rosgen 1989; Bloom 1991; Schick and Lekach 1993). If these same fractions are applied to the rivers in this study, the basin erosion rates will be significantly higher.

Summary and Conclusions

This study demonstrated the viability of using suspended sediment records as a means to estimate erosion rates, even in mountainous, tectonically active regions like Taiwan. Better estimates are obtained by recognizing the supply-limited nature of sediment supply by discrete events such as debris flows and landslides and correcting rating curve methods of erosion rate estimation. More complete data records yield better estimates using a rating curve method; less complete records appear to yield better erosion rate estimates from a simpler mean sediment discharge method. In the ECR of Taiwan, we obtained erosion rate estimates of 3.3–10.2 mm/yr from the mean sediment discharge method and estimates of 0.8–26.0 mm/yr from the corrected rating curve method. Using the preferred method for each basin, the estimates for erosion rates from the eastern Central Range are between 2.1 and 8.3 mm/yr.

To obtain a measure of the uncertainty in these erosion rate estimates as well as to try to understand the source of variation in the sediment discharge record, we constructed a stochastic model to predict the sediment discharge at a gauging station on the Chihpen River. This model contains a stochastic model for the rainfall and discharge in the river and a second stochastic component representing the sediment supplied to channels by landslides. Sediment transport was deterministic and used a physically based transport law and slope area data derived from a DEM. Unknown parameters for this model included cutoff values of the PDF for landslide magnitude, the transport coefficient in the suspended sediment transport law, and the dependence of landslide frequency on rainfall. These were all calibrated using the statistical characteristics of the observed sediment discharge record. It was also necessary to assume an erosion rate for the basin to calibrate the frequency of landslide occurrence, so this model is a tool to evaluate variability, not absolute rates. For the physical characteristics of the Chihpen River, a 27-yr record with 29/yr sampling frequency and an erosion rate of 5.1

mm/yr, we found that erosion rates for this river have a 68.3% probability of being within ± 2.7/4.0 mm/yr of the estimated erosion rate. A sampling frequency of 1/d would reduce that range to ±1.4/2.0 mm/yr, while a 100-yr record of daily observations would reduce the range to ±0.6/1 mm/yr.

ACKNOWLEDGMENTS

This study was supported by National Science Foundation grant EAR-9526954. We wish to thank C. Stark for his helpful comments regarding Pareto distributions and his thoughtful review and an anonymous reviewer for insightful comments.

REFERENCES CITED

Anderson, R. S. 1994. Evolution of the Santa Cruz Mountains, California, through tectonic growth and geomorphic decay. J. Geophys. Res. 99:20,161–20,179.

Barry, R. G., and Chorley, R. J. 1987. Atmosphere, weather, and climate (5th ed.). New York, Methuen, 460 p.

Benda, L., and Dune, T. 1997. Stochastic forcing of sediment supply to channel networks from landsliding and debris flow. Water Resour. Res. 33:2849–2863.

Bloom, A. 1991. Geomorphology: a systematic analysis of Late Cenozoic landforms. Englewood Cliffs, N.J., Prentice-Hall, 532 p.

Branski, J. 1981. Accuracy of estimating basin denudation processes from suspended sediment measurements. *In* Erosion and Sediment Transport Measurement, proceedings of the Florence symposium, June 1981. Washington, D.C., Int. Assoc. Hydrol. Sci. Publ. 133, p. 213–218.

Burbank, D. W.; Leland, J.; Fielding, E.; Anderson, R. S.; Brozovic, N.; Reid, M. R.; and Duncan, C. 1996. Bedrock incision, rock uplift and threshold hillslopes in the northwestern Himalayas. Nature 379:505–510.

Chang, C. P.; Angelier, J.; and Huang, C. Y. 2000. Origin and evolution of a mélange: the active plate boundary and suture zone of the Longitudinal Valley, Taiwan. Tectonophysics 325:43–62.

Chen, T. C.; Yen, M. C.; Hsieh, J. C.; and Arritt, R. W. 1999. Diurnal and seasonal variations of the rainfall measured by the automatic rainfall and meteorological telemetry system in Taiwan. Bull. Meteorol. Soc. 80:2299–2312.

Colby, B. R. 1956. Relationship of sediment transport to streamflow. U.S. Geol. Surv. Open-File Report, 170 p.

Dickinson, W. T. 1981. Accuracy and precision of suspended sediment loads. *In* Erosion and Sediment Transport Measurement, proceedings of the Florence symposium, June 1981. Washington, D.C., Int. Assoc. Hydrol. Sci. Publ. 133, p. 195–202.

Dorsey, R. J., and Lundberg, N. 1988. Lithofacies analysis and basin reconstruction of the Plio-Pleistocene collision basin, Coastal Range of eastern Taiwan. Acta Geol. Taiwan 26:57–132.

Ho, C. S. 1986. A synthesis of the geologic evolution of Taiwan. Tectonophysics 125:1–16.

Hovius, N. 1999. Macro scale process of mountain belt erosion. *In* Summerfield, M. A., ed. Global tectonics and geomorphology. New York, Wiley, p. 77–106.

Hovius, N.; Stark, C. P.; and Allen, P. A. 1997. Sediment flux from a mountain belt derived by landslide mapping. Geology 25:231–234.

Hovius, N.; Stark, C. P.; Chu, H. T.; and Lin, J. C. 2000. Supply and removal of sediment in a landslide-dominated mountain belt: Central Range, Taiwan. J. Geol. 108:73–89.

Inman, D. L., and Jenkins, D. L. 1999. Climate change and the episodicity of sediment flux of small Californian rivers. J. Geol. 107:251–270.

Li, Y. H. 1976. Denudation of Taiwan Island since the Pliocene Epoch. Geology 4:105–107.

Limpert, E.; Stahel, W. A.; and Abbt, M. 2001. Log-normal distributions across the sciences: keys and clues. BioScience 51:341–352.

Lin, C. H. 1998. Tectonic implications of an aseismic belt beneath the eastern central range of Taiwan: crustal subduction and exhumation. J. Geol. Soc. China 41:441–460.

Nanson, G. C. 1974. Bedload and suspended-load transport in a small, steep, mountain stream. Am. J. Sci. 274:471–486.

Nuttonson, M. Y. 1963. The physical environment and agriculture of central and south China, Hong Kong and Taiwan (Formosa). Washington, D.C., American Institute of Crop Ecology, 402 p.

Pearce, A. J., and McKerchar, A. I. 1979. Upstream generation of storm runoff. *In* Murray, D. L., and Ackroyd, P., eds. Physical hydrology: New Zealand experience. Wellington North, New Zealand Hydrological Society, p. 165–192.

Press, W. H.; Flanner, B. P.; Teukolsky, S. A.; and Vetterling, W. T. 1998. Numerical recipes in C. New York, Cambridge University Press, 994 p.

Qiwei, H.; Mingmin, H.; and Wang, S. S. Y. 1989. Two-dimensional nonequilibrium transport of nonuniform sediment. *In* Wang, S. S. Y., ed. Sediment transport modeling. New York, American Society of Civil Engineers, p. 572–580.

Ramage, C. S. 1971. Monsoon meteorology. New York, Academic Press, 269 p.

Rijn, L. C. 1984. Sediment transport. II. Suspended load transport. J Hydraulic Eng. 110:1613–1641.

Schick, A. P., and Lekach, J. 1993. An evaluation of two ten-year sediment budgets, Nahal, Israel. Phys. Geogr. 14:225–238.

Schmidt, K. M., and Montgomery, D. R. 1995. Limits to relief. Science 270:617–620.

Shelby, M. J. 1982. Hillslope materials and processes. Oxford, Oxford University Press, 264 p.
Stark, C. P., and Hovius, N. 2001. The characterization of landslide size distributions. Geophys. Res. Lett. 28: 1091–1094.
Tao, S., and Chen, L. 1987. A review of recent research on the East Asian summer monsoon in China. *In* Chang, C. P., and Krishnamurti, T. N., eds. Monsoon meteorology. Oxford, Oxford University Press, p. 60–92.
Tucker, G. E., and Bras, R. L. 2000. A stochastic approach to modeling the role of rainfall variability in drainage basin evolution. Water Resour. Res. 36:1953–1964.
Varnes, D. J. 1958. Landslide types and processes. *In* Eckel, E., ed. Landslides and engineering practices. Highway Res. Board Spec. Rep. 29:24–47.
Walling, D. E., and Webb, B. W. 1981. The reliability of suspended sediment load data. *In* Erosion and Sediment Transport Measurement, proceedings of the Florence symposium, June 1981. Washington, D.C., Int. Assoc. Hydrol. Sci. Publ. 133, p. 177–194.
Water Resources Planning Commission. 1972–1997. Hydrological year book of Taiwan, Republic of China. Taipei, Ministry of Economic Affairs, Taiwan.
———. 1973. Preliminary estimation of river sedimentation in Taiwan. Taipei, Ministry of Economic Affairs, Taiwan.
Williams, G. P., and Rosgen, D. L. 1989. Measured total sediment loads (suspended and bedloads) for 93 United States streams. U.S. Geol. Surv. Open-File Report 98–67, 128 p.
Yu, S. B.; Chen, H. Y.; and Kuo, L. C. 1997. Velocity field of GPS stations in the Taiwan area. Tectonophysics 274:41–59.